Bioorganic & Medicinal Chemistry 18 (2010) 6756–6762

Contents lists available at ScienceDirect

Bioorganic & Medicinal Chemistry

journal homepage: www.elsevier.com/locate/bmc

Studies on ligand binding to histidine triad nucleotide binding protein 1

Guoyun Bai, Bo Feng, Jia Bei Wang, Edwin Pozharski, Michael Shapiro *

University of Maryland, Department of Pharmaceutical Sciences, Baltimore, MD 21201, United States

ARTICLE INFO

Article history:
Received 18 May 2010
Revised 14 July 2010
Accepted 22 July 2010
Available online 27 July 2010

Keywords:
NMR
HINT1
Ligand–protein interactions
HSQC chemical shift mapping

ABSTRACT

Histidine triad nucleotide binding protein (HINT1) is an intracellular protein that binds purine mononucleotides. Strong sequence conservation suggests that these proteins play a fundamental role in cell biology, however its exact cellular function continues to remain elusive. nuclear magnetic resonance (NMR) studies using STD and HSQC were conducted to observe ligand binding to HINT1. These studies were confirmed using fluorescence spectroscopy titrations. We found that AICAR, the first non-phosphate containing ligand, binds to mouse histidine triad nucleotide binding protein 1 (HINT1). Chemical shift perturbations are mapped onto the X-ray structure showing AICAR binds at the same site as GMP. The NMR results demonstrated that this method will be valuable for the future screening of small molecules that can be used to modulate the function of HINT1.

1. Introduction

Histidine triad nucleotide binding protein 1 (HINT1) is a member of a superfamily of histidine triad (HIT) proteins named by the conserved nucleotide binding motif related to the sequence His-φ-His-φ-His-φφ, in which φ is a hydrophobic amino acid.[1,2] It was originally identified as protein kinase C interacting protein (PKCI-1),[3] but the PKC inhibitory activity could not be confirmed. The protein was renamed HINT1 based on the X-ray structural analysis which revealed that the protein has the same histidine triad motif as other HIT proteins. HINT1 is an intracellular protein that binds to purine mononucleotides, and while HINT protein is expressed in multiple tissues, especially abundant in brain, liver and kidney, its exact cellular function continues to remain nebulous.

Strong sequence conservation among species suggests that HINT proteins play a fundamental role in cell biology. It is present in both the nucleus and cytoplasm, and in the cytoplasm it is localized to cytoskeletal structures.[4] Recent research shows that HINT1 protein has tumor suppressor function through inhibiting transcription factor AP-1 activity or by interacting with Pontin and Reptin and inhibiting TCF-beta-catenin-mediated transcription.[5,6] It has been proposed that the phosphoramidase activity of HINTs is an important process for antiviral and anticancer phosphoramidate pro-nucleotides.

It has also been reported that mRNA expression of HINT1 was decreased in dorsolateral prefrontal cortex of schizophrenia patients compared with age and gender-matched controls.[7] This change was validated by real time quantitative polymerase chain reaction and in situ hybridization.[7] Association and expression studies suggest further that HINT1 gene is associated with schizophrenia and bipolar disorders and therefore is a potential drug target for mental disorders.

In previous studies, it was found that this protein is widely expressed in the mouse CNS with relatively high abundance in olfactory system, cerebral cortex, hippocampus and part of thalamus, midbrain, and medulla.[8] These results provide the anatomical evidence for the potential roles of HINT1 in neuronal function. It appears that HINT1 interacts with mu opioid receptor (MOR) and that this interaction leads to the suppression of MOR desensitization and PKC-related MOR phosphorylation and may also play a role in mediating the action of psycho-stimulants.[9,10] HINT1 deficiency leads to higher locomotor and stereotypic responses to the psychostimulant D-amphetamine in knockout (KO) mice as compared with wild type (WT) controls, likely through the dopaminergic system at the postsynaptic level. More recently it has been discovered that several phenotypes from HINT1 KO mice are characterized by the manifestation of bipolar disease. All of these studies suggest that HINT1 could play important roles in the neuropathology of these CNS diseases although details regarding the mechanisms of action for this protein are still not clear.

To understand this potentially important protein, it is necessary to have a stable molecular probe that can be used to study the pharmacological mechanism and modulate the protein's function and ultimately allow for an understanding of the function of HINT1 from the molecular, through the cellular and to the behavioral levels. Currently, these molecular tools do not exist.

Structurally, HINT1 consists of 126 amino acids, and is a homodimer which contains a 10-stranded anti-parallel β-sheet, five strands contributed by each monomer. Two identical nucleotide

* Corresponding author. Tel.: +1 410 660 9008.
E-mail address: mike6747@comcast.net (M. Shapiro).

0968-0896/$ - see front matter © 2010 Elsevier Ltd. All rights reserved.
doi:10.1016/j.bmc.2010.07.051

binding sites are seen and conserved hydrophobic residues create the binding site for the purine base and nonpolar and polar residues form the binding site for the ribose. Conserved polar residues, including His 110 and His 112 from the HIT motif, create the binding site for the α-phosphate.[11,12] Based upon the observation that five of the six completely conserved residues and 14 of the 26 highly conserved residues make direct contact with the nucleotide, it was suggested that HIT proteins constitute a new superfamily of nucleotide binding proteins. The discovery that bacterial and human HINTs are phosphoramidases, suggests the possibility of rational design of potential therapeutic nucleotide mimetics that can be targeted to diseased tissues. In vitro studies indicated that human HINT1 can bind various nucleotides, including AMP, ADP, and the diadenosine polyphosphates Ap3A and Ap4A.[11] It has been shown that rabbit HINT1 also binds several purine nucleosides and nucleoside phosphates.[13] Furthermore, the motifs in HINT1 which make contact with potential binding protein partners remains unidentified. The NMR studies presented here and more advanced three-dimensional structures using NMR and X-ray will provide the basis for addressing these questions.

Here we report the first NMR studies on HINT binding ligands, establishing the ground work for further rational drug design studies. NMR is one of the most valuable tools in the drug discovery to look for molecules that interact at the protein level and due to its ease of application to systems that have difficult or unknown functional assays, it provides an excellent screen for binding interactions.[14–17] The binding data found by NMR are compared with results obtained by X-ray crystallography for two ligands GMP and 5-aminoimidazole-4-carboxamide-ribonucleoside (AICAR). AICAR was selected as a trial ligand since it is a known nucleoside mimetic.[18,19] Our study is designed to establish an NMR method that will aid identification of chemical compounds that bind to HINT1 and therefore allow for structure based drug design.

2. Experimental

^{15}N Labeled and ^{15}N, ^{13}C double labeled HINT1 protein was prepared as previously described.[20] Unlabeled HINT1 protein was expressed in LB media instead of M9 media, and purified using the same methods. GMP, AICAR and phosphorylated AICAR were purchased from Sigma–Aldrich and used without further purification.

2.1. NMR spectroscopy

The NMR samples for ligand titration contain 0.2 mM ^{15}N labeled HINT1, 50 mM sodium phosphate, 50 mM NaCl, pH 7.3, in 90% H_2O and 10% D_2O. The backbone assignments of ^{1}H, ^{15}N and ^{13}C of apo HINT1 have been reported and been deposited in the BioMagResBank under BMRB accession number 15787.[20] The HINT1-ligand complex was generated by adding increasing amounts of ligand from a 50 mM solution for GMP or 20 mM for AICAR to a 0.2 mM HINT1, respectively. NMR data were obtained by $^{1}H–^{15}N$ two dimensional (2D) heteronuclear single quantum coherence (HSQC) spectra. The assignment of the $^{1}H–^{15}N$ HSQC spectra of GMP-HINT1 and AICAR-HINT1 complexes were obtained by the titration of ligands and confirmed by HNCACB spectra acquired on a sample containing 0.5 mM ^{15}N, ^{13}C doubly labeled protein and 4 mM GMP.

NMR spectra were recorded at 25 °C. $^{1}H–^{15}N$ HSQC spectra were recorded on a Bruker 600 using 1024 points and 128 increments. As an aid to the assignments, a HNCACB spectrum of HINT1-GMP complex was also recorded with 1024 points.[21] All the NMR data were processed and analyzed using the NMRPipe and NMRDraw software packages.[22]

1D Saturation transfer difference (STD) NMR was applied to samples of 0.1 mM unlabeled HINT1 protein with 2 mM of each ligand.[23] The mixture of 4 mM GMP and 4 mM AICAR without protein was used as a control. The spectra were recorded on Varian AS500 with 32 K points and 128 scans, with selective saturation of the protein resonances at 0.8 ppm for saturated spectra and −10 ppm for reference spectra interleaved, respectively, using a series of 60 Gaussian shaped pulses (50 ms, 1 ms delay between pulses), for a total saturation time of 3 s. The intensity of the selective saturation Gauss pulses corresponds to a field strength of 90 Hz.

2.2. Fluorescence

Binding affinity was determined for AICAR and GMP using quenching of the intrinsic Trp fluorescence of purified HINT1. Fluorescence measurement was carried out using a fluorimeter (Photon Counting Spectrofluorimeter, ISS) with the excitation wavelength at 295 nm and emission wavelength at 375 nm. The K_D fitting was carried out using nonlinear regression (GraphPad Prism4, GraphPad Software Inc.) using the equation below:[24]

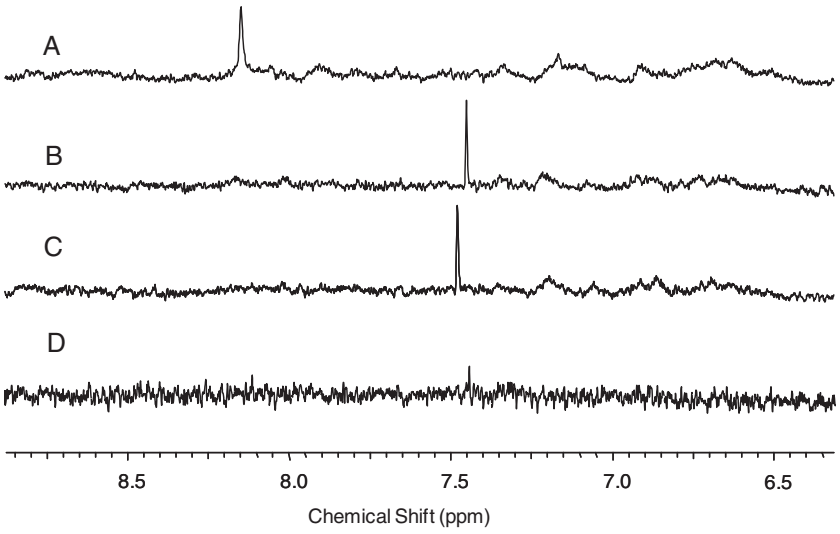

Figure 1. STD-NMR spectra of GMP (A), AICAR (B) and phosphorylated AICAR (C) binding to HINT1 after subtraction of unsaturated spectrum. The same procedure was applied to the mixture of GMP and AICAR in the absence of the protein as a control (D).

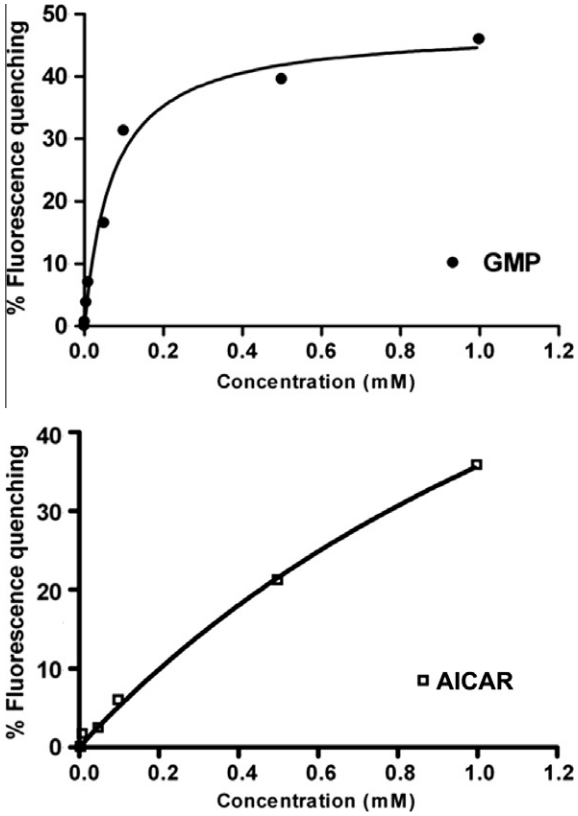

Figure 2. Quenching of HINT1 fluorescence by GMP and AICAR. Fluorescence data were fit to a one-site binding model using Eq. 1.

$$\left(\frac{\Delta F}{F_0}\times 100\right)=\frac{[S]\times\left(\frac{\Delta F_{max}}{F_0}\times 100\right)}{K_D+[S]} \quad (1)$$

where $(\Delta F/F_0 \times 100)$ is the percent fluorescence quenching following addition of ligand at a concentration [S], and K_D is the apparent dissociation constant.

Intrinsic Trp fluorescence of HINT1 (0.5 μM) was performed at 25 °C, in 0.5 ml 50 mM Tris–HCl buffer at pH 7.5, with 1 mM EDTA, 1 mM DTT and 5% glycerol, in a microcuvette with 5-mm optical pathlength. The concentrated ligand was titrated into the HINT1 solution stepwise. The inner filter effect was corrected by titrating the same concentration of ligand as used above into 0.5 μM *N*-acetyl-tryptophanamide.

2.3. X-ray crystallography

Crystallization conditions were determined by sparse matrix screening using Nextal Classics II crystallization screen from Qiagen (Valencia, CA). 100 nL of reservoir solution was mixed with 200 nL of 300 nL of HINT1/AICAR using Oryx Nano from Douglas Instruments (East Garston, UK). For cryo-protection the crystals were transferred to a drop of 2.5 M sodium malonate, pH 7.5, supplemented with 0.3 mM AICAR. After brief incubation, crystal was flash-cooled in liquid nitrogen. A native dataset at 1.45 Å resolution was collected at Stanford Synchrotron Radiation Lightsource, beamline 7–1. Structure was solved by molecular replacement using HINT1/N-ethylsulfamoyladenosine (PDB ID 1RZY) complex as a model. The detailed X-ray crystallography data will be presented in detail elsewhere. There were three copies in the asymmetric unit, for one and a half dimer (the third molecule was part of the dimer formed by crystal symmetry). The ligand-binding site is not at the interface.

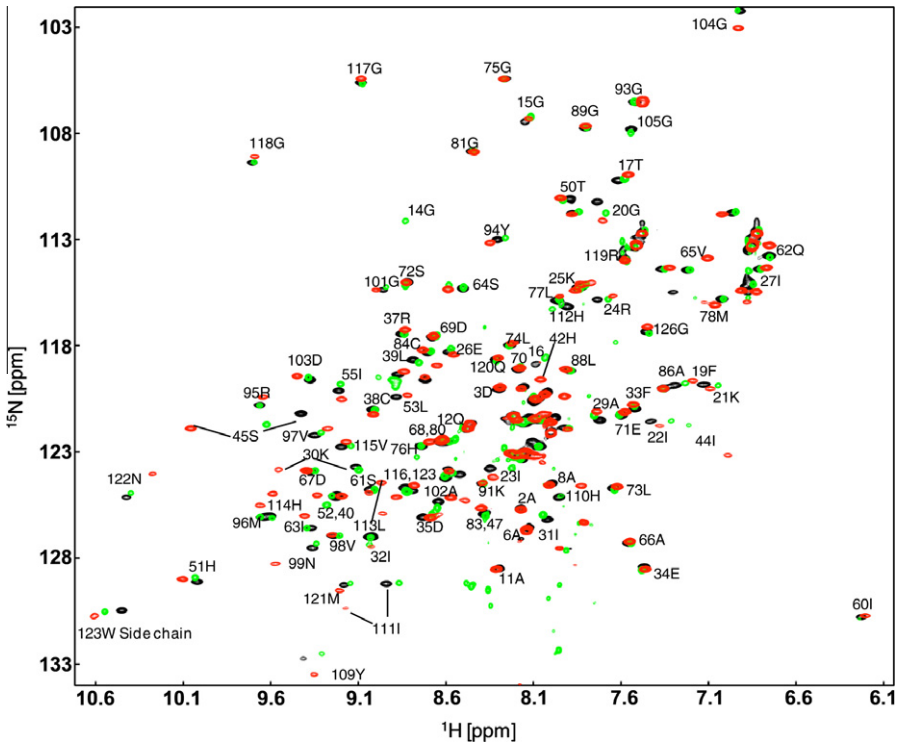

Figure 3. ^{1}H–^{15}N HSQC spectra of HINT1 (black) and HINT1 complexed with GMP (red) and AICAR (green).

3. Results

Saturation transfer difference (STD)-NMR spectroscopy was used to check for the binding of several ligands. STD NMR does not require isotope-labeled protein, can be worked with at low protein concentrations, and the results can be obtained in a relatively short time. Since GMP is a known HINT1 ligand with reasonable binding affinity, it was used here to validate the STD experiment.[13] In Figure 1 are shown the STD data for GMP (1A) as well as two other ligands AICAR phosphate (1B) and AICAR (1C). In the STD experiment, ligand binding was observed by the presence of the residual NMR signal, for example at $\delta = 8.18$ for GMP. Similar STD results were obtained for the AICAR ligands. The signals in the aliphatic region are obscured or distorted by water presaturation.

The binding was confirmed by fluorescence quenching experiments shown in Figure 2. The binding dissociation constant was calculated to be 1.1 ± 0.7 mM for AICAR and 67 ± 7.9 μM for GMP.

The binding site of the ligand was established using HSQC data from isotopically enriched protein. Since the signals on $^{1}H-^{15}N$ HSQC spectra of apo mouse HINT1 have been previously assigned in our laboratory,[20] the $^{1}H-^{15}N$ HSQC data allows assessment of binding at an atomic level. To this end, the spectra of HINT1 protein in the presence of GMP and AICAR were obtained and assigned, respectively. (Fig. 3) The chemical shift titration of HINT1 with AICAR and GMP is shown in Fig. 4. When the molar ratio of ligand to protein is 0.125, there are slight chemical shifts changes and these shifts increase as the concentration of AICAR is varied from 0.25, 0.5, 1, and 2.5 molar equivalents, respectively. Based upon the ^{1}H chemical shift perturbations using the equation below, it can be calculated that the K_D for AICAR is 1.2 ± 0.4 mM, which is in good agreement with the fluorescence data of 1.1 ± 0.7 mM:

$$\delta\ (\text{ppm}) = \delta_f - (\delta_b - \delta_f) \times \frac{(K_D + [L] + [P]) - \sqrt{(K_D + [L] + [P])^2 - 4[P][L]}}{2[P]} \quad (2)$$

where δ_f is the chemical shift when there is no ligand, δ_b is the chemical shift at saturation, [L] and [P] are the ligand and protein concentrations, respectively.[25]

Using the same methodology, the NMR data showed that the K_D for GMP was 60 ± 10 μM as shown in Figure 4.

For ease of comparison and to aid the elucidation of the binding site, the HSQC chemical shift changes with ligands GMP and AICAR are plotted against the linear sequence of HINT in Figure 5A. The values shown represent the combined chemical shift perturbations $\Delta\delta$ of both the ^{15}N and ^{1}H dimensions ($\Delta\delta_N$ and $\Delta\delta_H$, respectively) and was calculated using the equation:[26]

$$\Delta\delta\ (\text{ppm}) = \sqrt{(\Delta\delta_H)^2 + (0.154\Delta\delta_N)^2} \quad (3)$$

Shown in Figure 5B is a map of amino acid residues affected in the HINT1-GMP complex.

X-ray data was obtained on the HINT1-AICAR complex. This structure represents the first structure that has been obtained on a non-phosphate containing ligand. The details of this structure will be presented in a future report.

4. Discussion

In the evaluation of potential ligands for drug design, it is necessary to insure that the compounds of interest bind to the protein and that binding site is identifiable. In this study, it was established that ligand binding to HINT1 could be observed by NMR spectroscopy. It has been shown that STD NMR is a sensitive method to observe even very weak binding ligands to HINT1 and was successful in its application to AICAR (a nucleotide mimetic). While the fluorescence data also indicated this interaction, the advantage of an NMR screen is that it can be multiplexed for high-throughput and it does not suffer from the potential interferences such as seen in fluorescence data arising from the high concentrations of the ligand. $^{1}H-^{15}N$ HSQC spectra were used to monitor the chemical shift changes upon binding of the protein. Since the assignment of the backbone resonances was known from our previous work, a good indication on the location of the ligand was obtained.[20]

From a first glance, the HSQC spectrum seemed quite amenable to analysis as it represented well resolved peaks typical of β-sheet-like proteins. However, the peaks in the HSQC spectrum did appear broader than normal, even though the protein is only 13.8 KD. This additional broadening of the $^{1}H-^{15}N$ HSQC spectra is consistent with this protein being a dimer as was also observed from X-ray data.[11–13] It was found that the assignments of apo HINT1 is aided by evaluating the ligated state, where the overlapping signals become resolved in some areas of the spectrum. A good example of this effect is exemplified using the titration data for I44 (Fig. 6) which shows a very large chemical shift perturbation upon ligand binding. As can be seen in the apo HINT1 HSQC spectrum, this key

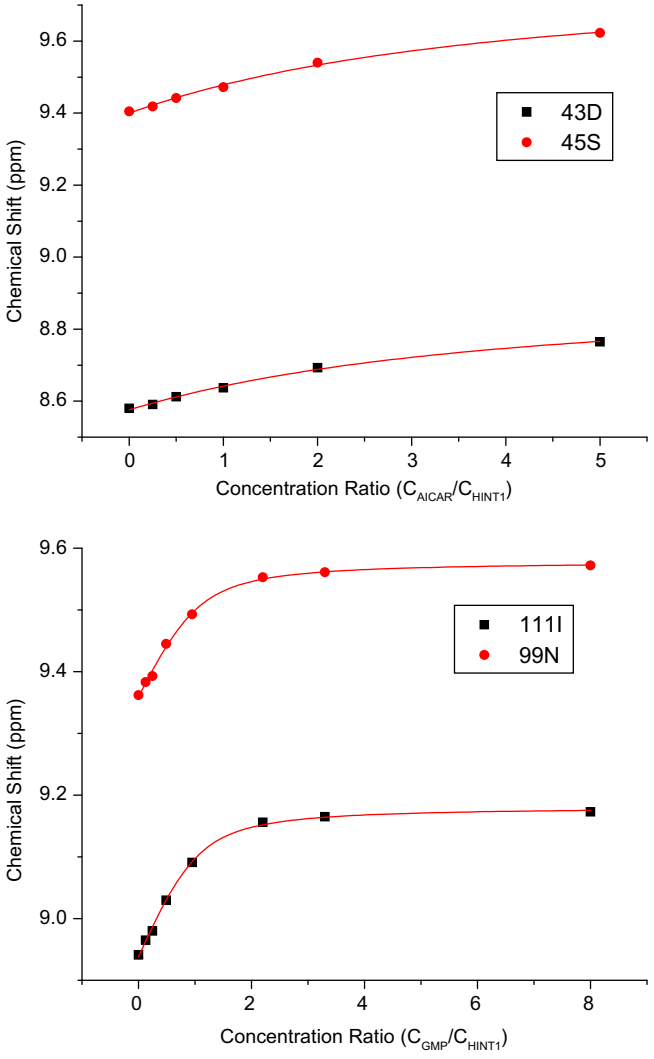

Figure 4. Binding curves for the interaction of HINT1 with GMP and AICAR. The amide ^{1}H chemical shifts of certain peptides at different ligand–protein ratios are shown. The data was fit to a single-site binding model using Eq. 2 in order to obtain the apparent dissociation binding constant K_D.

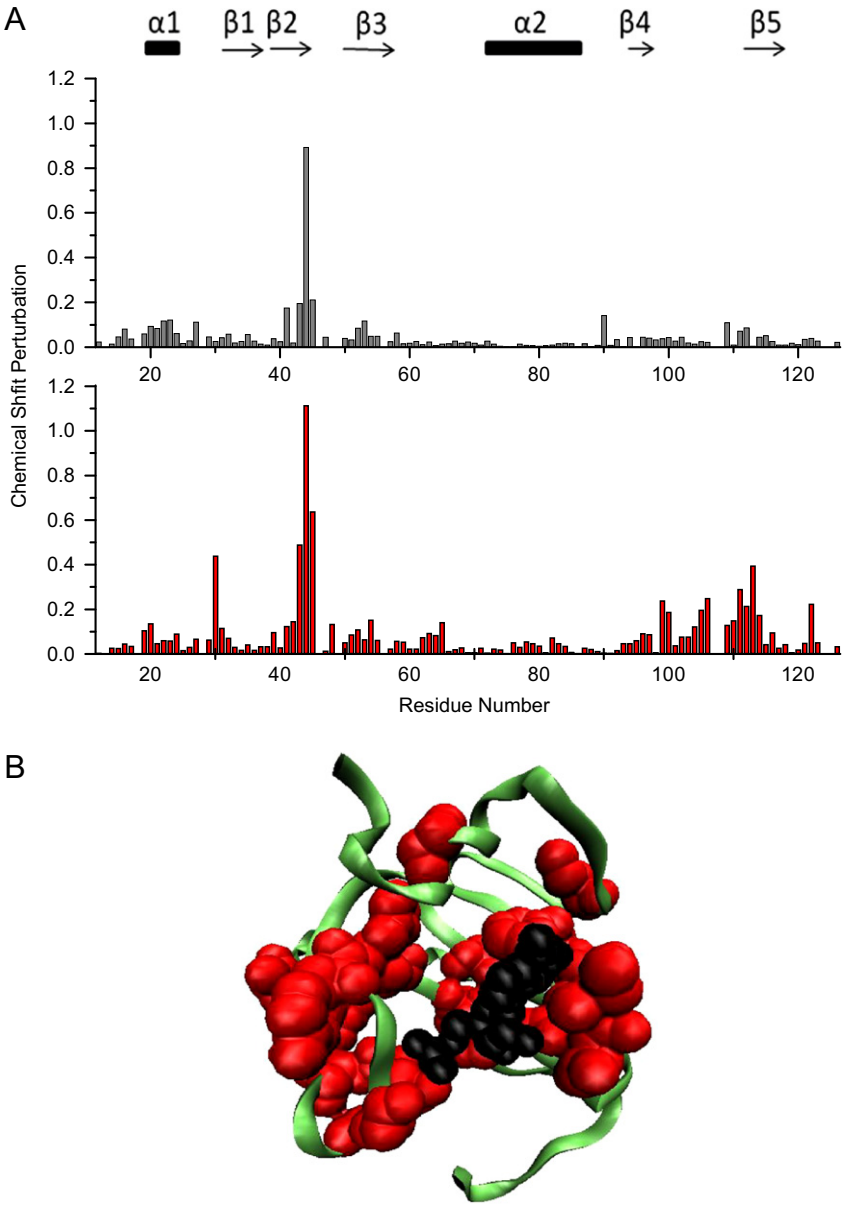

Figure 5. (A) NMR chemical shift perturbation calculated using Eq. 3 for AICAR (top) and GMP (bottom) relative to the linear sequence for HINT1. (B) Representation of the chemical shift perturbations upon binding ($\Delta\delta$ >0.1 ppm). Plotted in red balls are the residues affected mapped onto the X-ray structure of HINT1.

residue was not easy to resolve. It separates from the overlapping area after one equivalent of AICAR.

Spectra complexed to GMP yielded even more information than those of the AICAR–protein complex since the chemical shift changes were larger and many more of the buried peaks became visible. In order to ensure all amino acids and sequence assignments were correct, HNCACB spectra were collected. GMP bound states of HINT1 also allowed for higher quality HNCACB spectra, which might be due to the stabilization of the protein structure by ligand binding.

The GMP binding pocket of rabbit HINT1 protein has been previously revealed by crystal structure (PDB code 3RHN).[13] Based upon the X-ray data for GMP-HINT1 binding, it is expected that in the $^{1}H–^{15}N$ HSQC data a cluster of residues (shown in Figs. 3 and 5) should be highly sensitive to the addition of the nucleotide. The most pronounced chemical shift perturbations ($\Delta\delta$ >0.1 ppm) are observed for the residues of in or adjacent to strands β1, β2, β5 and helix α1, which form three sides of a canopy that holds the nucleotide on top of the β-sheet in accord with the crystal structure of rabbit HINT1 with GMP.[13] Residues 30 and 43–45 show the quite large chemical shift perturbations ($\Delta\delta$ >0.4 ppm). These residues are found in the binding pocket where the guanine and the sugar residues of GMP are located. Among these residues, Asp 43 is bound to the sugar OH group through two hydrogen bonds, which probably explains the large chemical shift perturbation ($\Delta\delta$ = 0.49 ppm). A relatively large chemical shift perturbation of $\Delta\delta$ = 0.15 ppm was observed for His 42. According to the X-ray, this residue is likely bound to the N2 amino group of the guanine through a hydrogen bond formed with its side chain OH group. Ile 44 shows the largest chemical shift difference of $\Delta\delta$ = 1.11 ppm, most likely due to its close proximity to the ligand. Residues such as 99, 106, 109–114 also show chemical shift perturbations. They are involved in the interactions with sugar and 5'-phosphate groups of GMP. Based upon these observations, the structural conclusions drawn from the NMR data is in agreement with the X-ray data obtained on the rabbit HINT1–GMP complex.

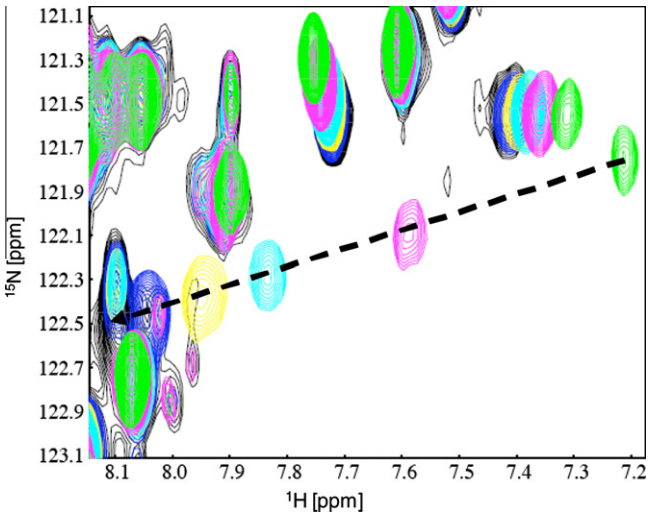

Figure 6. Expanded overlapping $^{1}H–^{15}N$ HSQC spectra of HINT1 with successive addition of AICAR. The concentration ratio (AICAR/HINT1) is 0 (black), 0.25 (blue), 1 (yellow), 2 (cyan), 5 (magenta) and 10 (green). The arrow shows the position of the hidden signal.

The binding of AICAR to HINT1 mapped to the linear sequence shown in Figure 5, reveals great chemical shift perturbation similarity as GMP indicating that the two ligands probably bind in the same basic location. It is worth noticing that residues at β5 such as Q106, I111 and H114 didn't show significant chemical shift changes in the AICAR spectrum which is consistent with the absence of 5'-phosphate. The X-ray structure of HINT1–AICAR was obtained and the nucleotide mimetic can be seen to bind to the same site as GMP (Fig. 7, detailed data to be placed in the PDB at a later date).

According to X-ray data of HINT1-AICAR complex, there are 4 hydrogen bonds formed by 3 residues (Ile 44, Asp 43, and Ser 107) with AICAR. The residues involved in the hydrophobic binding to AICAR are not exactly the same as GMP which is also consistent with the NMR chemical shift perturbation data. The biggest differences seen between the X-ray data for GMP and for AICAR are that there is a hydrogen bond formed by Ile 44 backbone with the AICAR N2 amino group and the interaction of the ribose C_5 hydroxyl group with Ser 107. The dramatic chemical shift perturbation ($\Delta\delta$ = 0.89 ppm) reflects this binding interaction very well. In the case of AICAR, His 42 is not involved in ligand binding; hence, the chemical shift perturbation is quite small. In addition it appears as though both Ile 22 and Ile 23 are involved in hydrophobic contact with ligand, which was not observed in GMP binding.

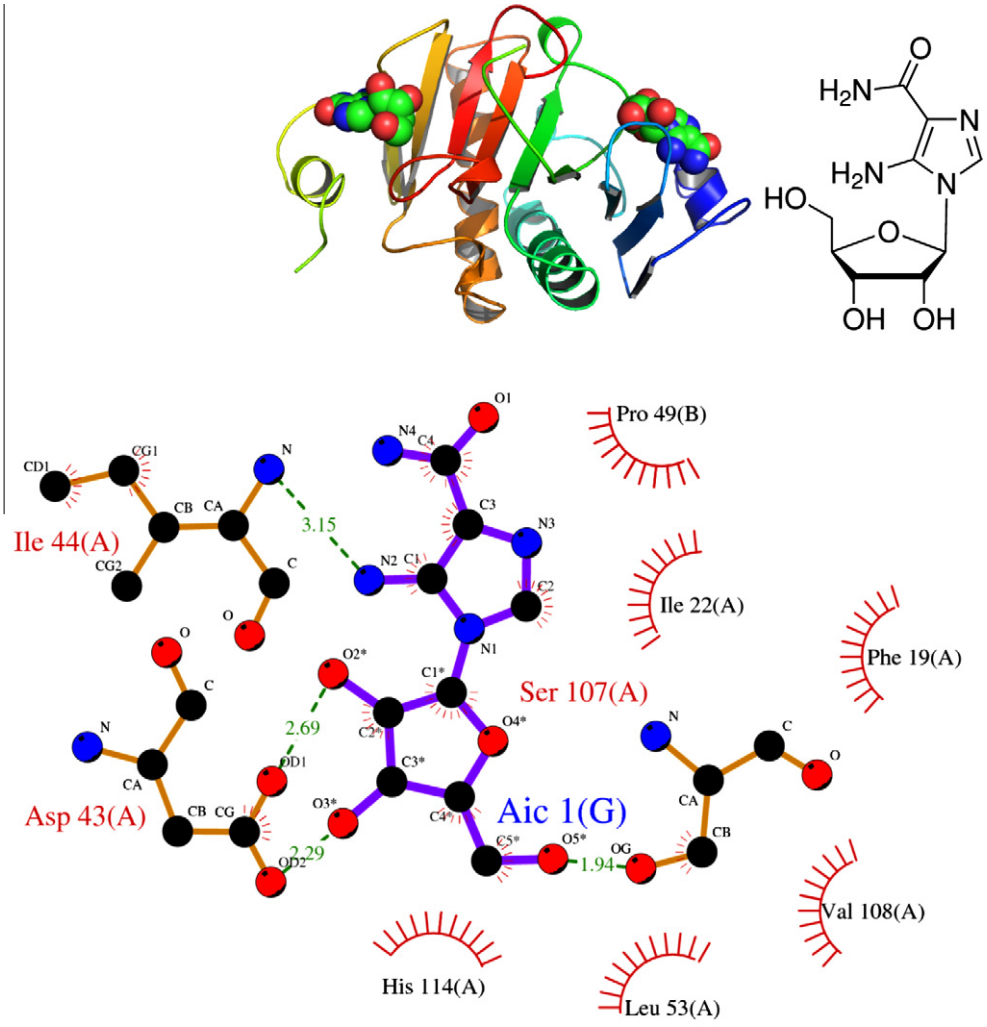

Figure 7. X-ray crystallography interaction map of the binding site of HINT1 and AICAR. The interaction map was generated using LIGPLOT.[27] In the upper corner is a ribbon diagram generated for the crystal structure of the HINT1-AICAR.

Even though the NMR chemical shift perturbation and X-ray data upon binding are generally in good agreement, there are some additional residues that stand out as showing different interactions. The NMR is very sensitive to binding events and residues near the binding sites generally have large chemical shift perturbations. According to the X-ray data, residue Ser 45 is not directly involved in a binding interaction, but it has relatively large chemical shift perturbation ($\Delta\delta$ = 0.21 ppm). We feel that this may be due to a secondary interaction effect perturbing its chemical shift, since there is a large interaction of the ligand with the adjacent residue Ile 44.

Both the X-ray and NMR studies show that certain residues involved in the binding activity with nucleotides are actually a majority of the most highly conserved residues in the HIT superfamily. It suggests that the conserved function of these proteins must depend on binding nucleotide. For tools to study this protein more effectively, the presence of the phosphate makes GMP and other derivatives poor drug candidates. AICAR and analogs might be a good alternative since they do not contain phosphate and they interact at the same binding site as GMP. Our study has established a method that will aid the identification of chemical compounds that bind to HINT1. The successful identification of nucleotides and a measurement of NMR data for a weakly binding nucleoside analog (AICAR) indicates the suitability of the approach.

References and notes

1. Klein, M. G.; Yao, Y.; Slosberg, E. D.; Lima, C. D.; Doki, Y.; Weinstein, I. B. *Exp. Cell Res.* **1998**, *244*, 26.
2. Seraphin, B. *DNA Seq.* **1992**, *3*, 177.
3. McDonald, J. R.; Walsh, M. P. *Biochem. Biophys. Res. Commun.* **1985**, *129*, 603.
4. Brzoska, P. M.; Chen, H.; Levin, N. A.; Kuo, W. L.; Collins, C.; Fu, K. K.; Gray, J. W.; Christman, M. F. *Genomics* **1996**, *36*, 151.
5. Wang, L.; Zhang, Y.; Li, H.; Xu, Z.; Santella, R. M.; Weinstein, I. B. *Cancer Res.* **2007**, *67*, 4700.
6. Weiske, J.; Huber, O. *J. Cell Sci.* **2005**, *118*, 3117.
7. Vawter, M. P.; Shannon Weickert, C.; Ferran, E.; Matsumoto, M.; Overman, K.; Hyde, T. M.; Weinberger, D. R.; Bunney, W. E.; Kleinman, J. E. *Neurochem. Res.* **2004**, *29*, 1245.
8. Liu, Q.; Puche, A. C.; Wang, J. B. *Neurochem. Res.* **2008**, *33*, 1263.
9. Chen, Q.; Wang, X.; O'Neill, F. A.; Walsh, D.; Kendler, K. S.; Chen, X. *Schizophr. Res.* **2008**, *106*, 200.
10. Guang, W.; Wang, H.; Su, T.; Weinstein, I. B.; Wang, J. B. *Mol. Pharmacol.* **2004**, *66*, 1285.
11. Lima, C. D.; D'Amico, K. L.; Naday, I.; Rosenbaum, G.; Westbrook, E. M.; Hendrickson, W. A. *Structure* **1997**, *5*, 763.
12. Lima, C. D.; Klein, M. G.; Weinstein, I. B.; Hendrickson, W. A. *Proc. Natl. Acad. Sci. U.S.A.* **1996**, *93*, 5357.
13. Brenner, C.; Garrison, P.; Gilmour, J.; Peisach, D.; Ringe, D.; Petsko, G. A.; Lowenstein, J. M. *Nat. Struct. Biol.* **1997**, *4*, 231.
14. Shapiro, M. *Farmaco* **2001**, *56*, 141.
15. Shapiro, M. J.; Wareing, J. R. *Curr. Opin. Drug Disc. Dev.* **1999**, *2*, 396.
16. Zartler, E. R.; Shapiro, M. J. *Curr. Pharm. Des.* **2006**, *12*, 3963.
17. Vogtherr, M.; Fiebig, K. *EXS* **2003**, 183.
18. Foley, J. M.; Adams, G. R.; Meyer, R. A. *Am. J. Physiol.* **1989**, *257*, C488.
19. Sajan, M. P.; Bandyopadhyay, G.; Miura, A.; Standaert, M.; Nimal, S.; Longnus, S. L.; Van Obberghen, E.; Hainault, I.; Foufelle, F.; Kahn, C. R.; Braun, U.; Leitges, M.; Farese, R. V. *Am. J. Physiol. Endocrinol. Metab.* **2009**, *12*, 23.
20. Bai, G.; Feng, B.; Wang, J. B.; Varney, K. M.; Shapiro, M. *Biomol. NMR Assign.* **2009**, *3*, 57.
21. Wittekind, M. *J. Magn. Reson., Ser. B* **1993**, *101*, 201.
22. Delaglio, F.; Grzesiek, S.; Vuister, G. W.; Zhu, G.; Pfeifer, J.; Bax, A. *J. Biomol. NMR* **1995**, *6*, 277.
23. Mayer, M.; Meyer, B. *Angew. Chem., Int. Ed.* **1999**, *38*, 1784.
24. Kalnik, M. W.; Kouchakdjian, M.; Li, B. F.; Swann, P. F.; Patel, D. J. *Biochemistry* **1988**, *27*, 108.
25. Morton, C. J.; Pugh, D. J. R.; Brown, E. L.; Kahmann, J. D.; Renzoni, D. A. C.; Campbell, I. D. *Structure* **1996**, *4*, 705.
26. Tugarinov, V.; Kay, L. E. *J. Mol. Biol.* **2003**, *327*, 1121.
27. Wallace, A. C.; Laskowski, R. A.; Thornton, J. M. *Protein Eng.* **1995**, *8*, 127.